Robust Control of Electro-Hydraulic Systems Subject to Input Constraints

Sule Taskingollu[1], Erman Selim[1,2], Alper Bayrak[3], Enver Tatlicioglu[1⋆] and Erkan Zergeroglu[4]

***Abstract*— This work presents a robust, neural network based controller formulation for the displacement tracking problem of electro–hydraulic systems subject to uncertainties associated with their dynamical parameters and actuator saturation. Specifically, a neural network based compensator is utilized to estimate some of the nonlinear components of the uncertain dynamical terms and then in conjunction with robust backstepping procedure, the overall formulation ensure the uniform practical stability of the closed–loop system. Stability and convergence of error terms are proven using Lyapunov based arguments and numerical studies are presented in order to illustrate the feasibility of the proposed methodology.**

I. Introduction

The use of electro-hydraulic systems (EHSs) is common in many areas, especially heavy industry where high power is required. These actuators are widely used in industrial applications, construction machinery, in the field of robotics, etc. The primary motivation for their usage is due to their ability to generate high power-to-weight ratio making it an ideal solution for lifting heavy loads. Their fast response time also enables them to perform tasks quickly and efficiently.

However, due to the complex flow characteristics of the servo valves within the hydraulic system, EHSs exhibit significant nonlinearities in their dynamics [1]. These characteristics have motivated engineers and researchers to concentrate on position control of EHSs. To name a few, [2] proposed an adaptive backstepping controller that tackled model uncertainties. In [3], authors proposed an output feedback nonlinear controller for the position tracking problem of EHSs. In [4], a high-gain observer based on a nonlinear backstepping control method is designed for tracking of a desired displacement signal.

While several aspects of EHSs have been studied, it seems that nonlinearities associated with the actuator saturation of EHSs are usually overlooked in the relevant literature. That is, in real life industrial applications EHSs are, most of the time, subject to actuator saturation. And any realistic model should consider the nonlinearity associated with the physical limitations of the electro-hydraulic actuator. However, to our surprise, there are only a few relevant studies that target this major problem. In [5], Guo *et al.* proposed a saturated adaptive controller for electro-hydraulic actuators to balance between the anti-windup control effect and the dynamic response performance of the EHS. In [6], Ye *et al.* presented a model-based commander filtering controller with a Nussbaum function to handle input saturation. [7] presented a disturbance observer-based fixed-time event-triggered controller for a networked EHS that is under the influence of input saturation nonlinearity.

The focus of this work is to design a position trajectory tracking controller for EHSs subject to modeling anomalies such as parameter uncertainties and nonlinearities associated with actuator saturation. To deal with the modeling uncertainties, a robust backstepping control approach is proposed. The part of the control input that is outside the limits of the actuator is then considered to be modeled with neural networks. The neural network compensation term is then integrated into the robust controller to remedy actuator saturation nonlinearity. The stability of the closed–loop system is investigated via Lyapunov based approach where the stability of the closed–loop system and uniform ultimate boundedness of the error signals are ensured. Specifically, the tracking error is guaranteed to be driven to a small region around the origin whose size can be adjusted via the controller gains. Comparative numerical simulations performed using realistic system parameters with and without neural network compensation terms are presented in order to illustrate the feasibility and performance of the proposed method.

The rest of this paper is organized in the following manner: The system model description is in Section II. The error system development and control input design are presented in Section III. The stability analysis is given in Section IV. Section V contains numerical simulation. Finally, conclusions are provided in Section VI.

II. System Model

The third order dynamic model of an EHA (electro-hydraulic actuator) can be represented as follows [1]

$$m\ddot{y} = -b\dot{y} - ky + A_p p_L - F_L \tag{1}$$

$$\dot{p}_L = -\frac{4\beta_e A_p}{V_t}\dot{y} - \frac{4\beta_e C_{tl}}{V_t}p_L + \frac{4\beta_e C_d \omega}{V_t\sqrt{\rho}}\,\mathrm{sat}(u)\sqrt{p_s - p_L\,\mathrm{sgn}(u)} \tag{2}$$

[1]Sule Taskingollu, Erman Selim, Enver Tatlicioglu are with the Department of Electrical and Electronics Engineering, Ege University, Izmir, Türkiye 91230000465@ogrenci.ege.edu.tr, erman.selim@ege.edu.tr, enver.tatlicioglu@ege.edu.tr

[2]Erman Selim is also with the Department of Mechanical and Mechatronics Engineering, University of Waterloo, Waterloo, ON, Canada. erman.selim@uwaterloo.ca

[3]Alper Bayrak is with the Department of Electrical and Electronics Engineering, Bolu Abant Izzet Baysal University, Bolu, Türkiye. alperbayrak@ibu.edu.tr

[4]Erkan Zergeroglu is with the Department of Computer Engineering, Gebze Technical University, Kocaeli, Türkiye. e.zerger@gtu.edu.tr

where the state vector is $\mathbf{x} = [x_1(t) \;\; x_2(t) \;\; x_3(t)] = [y(t) \; \dot{y}(t) \; p_L] \in \mathbb{R}^3$ in which $y(t)$ is the displacement, $\dot{y}(t)$ is the velocity, $p_L(t)$ is the load pressure and $u(t)$ is the spool position of the servo valve which serves as the control input. The control input u is considered to be subject to actuator saturation nonlinearity which is quantified with $\text{sat}(u)$ where the control input is constrained as $u_l \leq u \leq u_u$ with u_l and u_u respectively denoting lower and upper limits of the control input. The descriptions of the model parameters in (1) and (2) are listed in Table I.

TABLE I

MODEL PARAMETERS OF THE EHA SYSTEM

Parameter	Description
m	Load mass
b	Viscous damping coefficient
k	Load spring constant
A_p	Annulus area of the symmetrical chamber
F_L	External load of the hydraulic actuator
β_e	Effective bulk modulus
V_t	Half-volume of the cylinder
C_{tl}	Total leakage coefficient of the cylinder
C_d	Discharge coefficient
ω	Area gradient of the servo valve spool
ρ	Density of the hydraulic oil
p_s	Supply pressure

For ease of presentation, following auxiliary terms $\theta_{z0}(p_L, u)$, θ_{z1}, θ_{z2}, θ_{z3} are defined

$$\theta_{z0}(p_L, u) \triangleq \sqrt{p_s - p_L \,\text{sgn}(u)}, \tag{3}$$

$$\theta_{z1} \triangleq \frac{V_t\sqrt{\rho}}{4\beta_e C_d \omega}, \tag{4}$$

$$\theta_{z2} \triangleq \frac{A_p\sqrt{\rho}}{C_d \omega}, \tag{5}$$

$$\theta_{z3} \triangleq \frac{C_{tl}\sqrt{\rho}}{A_p C_d \omega}. \tag{6}$$

Using the definitions of (3)-(6), the dynamics of p_L in (2) can be rewritten as

$$\theta_{z1}\dot{p}_L = -\theta_{z2}\dot{y} - \theta_{z3}p_L + \theta_{z0}\,\text{sat}(u). \tag{7}$$

As the control input is subject to saturation nonlinearity, the part of the control input that cannot be applied by the electro-hydraulic actuator is represented with $\delta(t)$ and is defined as follows

$$\delta \triangleq u - \text{sat}(u) \tag{8}$$

In lieu of (8), (7) is further rearranged as follows

$$\theta_{z1}\dot{p}_L = -\theta_{z2}\dot{y} - \theta_{z3}p_L + \theta_{z0}u - \bar{\delta} \tag{9}$$

where $\bar{\delta}(t)$ is defined as

$$\bar{\delta} \triangleq \theta_{z0}\delta. \tag{10}$$

III. ERROR SYSTEM DEVELOPMENT AND CONTROL INPUT DESIGN

The objective is to ensure that the actuator tracks the desired position despite uncertain parameters while also dealing with saturation nonlinearity. The subsequent development relies upon the availability of the measurements of displacement y, velocity $\dot{y}$, load pressure p_L and thus θ_{z0} introduced in (3) is a measurable quantity. The desired position is represented with $y_d(t)$ and is considered to remain bounded up to its third order time derivative.

To assess the tracking control objective, tracking error, denoted by $e(t) \in \mathbb{R}$ is defined as

$$e \triangleq y_d - y, \tag{11}$$

and an auxiliary error term, denoted by $r(t) \in \mathbb{R}$, is defined as

$$r = \dot{e} + k_e e \tag{12}$$

where $k_e \in \mathbb{R}^+$ is a constant control gain. Differentiating (12), multiplying with $\frac{m}{A_p}$, and then utilizing (1), the following expression can be obtained

$$\frac{m}{A_p}\dot{r} = f_r - e - p_L \tag{13}$$

where $f_r(e, r, y_d, \dot{y}_d, \ddot{y}_d, t) \in \mathbb{R}$ is an auxiliary uncertain variable defined as follows

$$f_r \triangleq \frac{k}{A_p}y_d + \frac{b}{A_p}\dot{y}_d + \frac{m}{A_p}\ddot{y}_d + \frac{1}{A_p}F_L + \frac{mk_e - b}{A_p}r + \left(\frac{bk_e}{A_p} - \frac{mk_e^2}{A_p} - \frac{k}{A_p} + 1\right)e. \tag{14}$$

The above given function can be upper bounded as

$$|f_r| \leq \rho_r \tag{15}$$

with $\rho_r(|e|, |r|, t) \in \mathbb{R}$ being a known, positive bounding function.

To continue with the design, the backstepping error, shown with $z(t)$, is defined as

$$z \triangleq p_L - p_{Ld} \tag{16}$$

where $p_{Ld}(t) \in \mathbb{R}$ is to be designed virtual controller. Substituting (16) into (13) yields

$$\frac{m}{A_p}\dot{r} = f_r - e - z - p_{Ld}. \tag{17}$$

The virtual controller is designed as follows

$$p_{Ld} = k_r r + \frac{\rho_r^2}{\rho_r |r|_\xi + \epsilon_r} r \tag{18}$$

where $\epsilon_r \in \mathbb{R}$ is a small positive constant, and $|\cdot|_\xi$ is an absolute value type function introduced to ensure differentiability that is essential for the subsequent development and is defined as $|r|_\xi \triangleq \sqrt{r^2 + \xi} - \sqrt{\xi}$ for some positive constant ξ. By substituting (18) into (17), the closed loop dynamics is obtained as

$$\frac{m}{A_p}\dot{r} = f_r - e - z - k_r r - \frac{\rho_r^2}{\rho_r |r|_\xi + \epsilon_r} r. \tag{19}$$

By differentiating (16) and multiplying both sides with θ_{z1} and substituting the load pressure dynamics in (9), the following expression is obtained

$$\theta_{z1}\dot{z} = f_z + r + \theta_{z0}u - \bar{\delta} \tag{20}$$

where $f_z(e, r, z, y_d, \dot{y}_d, \ddot{y}_d, t) \in \mathbb{R}$ is defined as

$$f_z \triangleq -\theta_{z2}\dot{y}_d - \theta_{z1}\dot{p}_{Ld} - \theta_{z2}k_e e + (\theta_{z2} - \theta_{z3}k_r - 1)\, r - \theta_{z3} z. \quad (21)$$

The above function can be upper bounded as

$$|f_z| \leq \rho_z \quad (22)$$

with $\rho_z(|e|, |r|, |z|, t) \in \mathbb{R}$ being a known, positive bounding function.

Property 1. *Via utilizing the universal approximation property of neural networks [8], [9], [10], [11], the auxiliary term $\bar{\delta}$ can be modeled as*

$$\bar{\delta} = w\sigma + \epsilon \quad (23)$$

where $w \in \mathbb{R}$ denotes the constant weight, $\sigma(z) \in \mathbb{R}$ is the activation function, and $\epsilon(t) \in \mathbb{R}$ is the functional reconstruction error. It is noted that $|w| \leq \bar{w}$ and $|\epsilon(t)| \leq \bar{\epsilon}$ are satisfied for positive constants $\bar{w}$, $\bar{\epsilon}$.

After substituting the neural network approximation of (23) into (20), following expression is obtained

$$\theta_{z1}\dot{z} = f_z + r + \theta_{z0}u - w\sigma - \epsilon. \quad (24)$$

Based on error system development and subsequent stability analysis, the control input is designed as

$$u = \frac{1}{\theta_{z0}}\left(-k_z z - \frac{\rho_z^2}{\rho_z|z| + \epsilon_z} z + \hat{\bar{\delta}}\right) \quad (25)$$

where $\hat{\bar{\delta}}(t)$ is the neural network based compensation term that is designed as

$$\hat{\bar{\delta}} = \hat{w}\sigma \quad (26)$$

where $\hat{w}(t) \in \mathbb{R}$ is estimated weight updated according to

$$\dot{\hat{w}} = -\gamma_w \sigma z - k_w \gamma_w |z| \hat{w} \quad (27)$$

where γ_w, $k_w \in \mathbb{R}$ are positive adaptation gains. Upon substituting (25) and (26) into (24), the closed loop error dynamics is reached as

$$\theta_{z1}\dot{z} = -k_z z + r + f_z - \frac{\rho_z^2}{\rho_z|z| + \epsilon_z} z - \tilde{w}\sigma - \epsilon \quad (28)$$

where $\tilde{w}(t) \triangleq w - \hat{w} \in \mathbb{R}$ is the estimation error.

IV. Stability Analysis

Theorem 1. *The controller designed in* (25) *with the neural network based compensator designed as* (26) *and the online generated weight in* (27) *ensure the boundedness of the closed loop system and uniform ultimate boundedness of the tracking error provided that the controller gain k_z satisfy the following condition*

$$k_z = \kappa_z + k_n \bar{\epsilon}^2 + \frac{1}{16} k_n k_w^2 \bar{w}^4 \quad (29)$$

where κ_z is an auxiliary constant, positive control gain and k_n is a positive damping gain.

Proof: To prove the theorem, following non-negative function $V(e, r, z, \tilde{w}) \in \mathbb{R}$ is defined

$$V \triangleq \frac{1}{2}e^2 + \frac{m}{2A_p}r^2 + \frac{\theta_{z1}}{2}z^2 + \frac{1}{2\gamma_w}\tilde{w}^2. \quad (30)$$

Following bounds can be obtained for (30)

$$b_1 \|q\|^2 \leq V \leq b_2 \|q\|^2 + b_3 \quad (31)$$

where $q(t) \triangleq [e, r, z]^T \in \mathbb{R}^3$ is the combined error vector and b_1, b_2 and b_3 are positive bounds, defined as

$$b_1 \triangleq \frac{1}{2}\min\{1, \frac{m}{A_p}, \theta_{z1}\} \quad (32)$$

$$b_2 \triangleq \frac{1}{2}\max\{1, \frac{m}{A_p}, \theta_{z1}\} \quad (33)$$

$$b_3 \triangleq \frac{1}{2\gamma_w}\bar{\tilde{w}}^2 \quad (34)$$

with $\bar{\tilde{w}} \geq |\tilde{w}(t)|$ being utilized for some known positive constant $\bar{\tilde{w}}$ which can be ensured upon utilizing a projection algorithm (such as in [12], [13], [14]) along with (27).

Taking the time derivative of (30) and then substituting (12), (19), (27), (28), following expression is obtained

$$\dot{V} = -k_e e^2 - k_r r^2 - k_z z^2 - \epsilon z + k_w |z| \tilde{w}\hat{w} + r f_r - \frac{\rho_r^2}{\rho_r |r|_\xi + \epsilon_r} r^2 + z f_z - \frac{\rho_z^2}{\rho_z |z| + \epsilon_z} z^2. \quad (35)$$

From (15) and (22), following bounds can be reached

$$r f_r - \frac{\rho_r^2}{\rho_r |r|_\xi + \epsilon_r} r^2 \leq \rho_r |r| - \frac{\rho_r^2 r^2}{\rho_r |r| + \epsilon_r} \leq \epsilon_r \quad (36)$$

$$z f_z - \frac{\rho_z^2}{\rho_z |z| + \epsilon_z} z^2 \leq \rho_z |z| - \frac{\rho_z^2 z^2}{\rho_z |z| + \epsilon_z} \leq \epsilon_z \quad (37)$$

where in obtaining (36), $|r|_\xi \leq |r|$ is utilized. The boundedness of the functional reconstruction error, given in Property 1, along with Young's inequality yield the following expression

$$\epsilon z \leq \bar{\epsilon}|z| \leq \frac{1}{4k_n} + k_n \bar{\epsilon}^2 z^2. \quad (38)$$

The last term on the first line of the right hand side of (35) can be manipulated as follows

$$\tilde{w}\hat{w} = \tilde{w}w - \tilde{w}^2 \leq \bar{w}|\tilde{w}| - |\tilde{w}|^2 = -\left(\frac{\bar{w}}{2} - |\tilde{w}|\right)^2 + \frac{\bar{w}^2}{4} \leq \frac{\bar{w}^2}{4} \quad (39)$$

where $\bar{w}$ was introduced in Property 1. Using Young's inequality, following upper bound can be reached

$$\frac{1}{4}k_w \bar{w}^2 |z| \leq \frac{1}{4k_n} + \frac{1}{16}k_n k_w^2 \bar{w}^4 z^2. \quad (40)$$

Substituting (36)-(40) into the right hand side of (35), following upper bound is obtained

$$\dot{V} \leq -k_e e^2 - k_r r^2 + \epsilon_n - \left(k_z - k_n \bar{\epsilon}^2 - \frac{1}{16}k_n k_w^2 \bar{w}^4\right) z^2 \quad (41)$$

where $\epsilon_n \in \mathbb{R}^+$ is an auxiliary constant defined as follows

$$\epsilon_n \triangleq \epsilon_r + \epsilon_z + \frac{1}{2k_n}. \quad (42)$$

After substituting the control gain designed in (29), a further upper bound can be obtained for the right hand side of (41) as

$$\begin{aligned} \dot{V} &\leq -k_e\|e\|^2 - k_r\|r\|^2 - \kappa_z\|z\|^2 + \epsilon_n, \quad (43) \\ &\leq -\kappa_q\|q\|^2 + \epsilon_n \quad (44) \end{aligned}$$

where $\kappa_q \triangleq \min\{k_e, k_r, \kappa_z\}$.

From (31) and (44), the following expression can be reached

$$\dot{V} \leq -b_4 V + b_5 \quad (45)$$

where b_4 and b_5 are positive constants defined as

$$b_4 \triangleq \frac{\kappa_q}{b_2} \quad (46)$$

$$b_5 \triangleq \frac{\kappa_q b_3}{b_2} + \epsilon_n. \quad (47)$$

From (45), it follows that $V \in \mathcal{L}_\infty$, and thus, the error signals e, r, z and $\tilde{w}$ are also bounded. Standard signal chasing techniques can then be utilized to illustrate the boundedness of the closed–loop signals including the virtual control signal p_{Ld} and the control signal u.

Furthermore, the solution of (45) is obtained as

$$V(t) \leq V(0)\exp(-b_4 t) + \frac{b_5}{b_4}(1 - \exp(-b_4 t)), \quad (48)$$

therefore it is straight forward to conclude that, V approaches the ultimate bound of $\frac{b_5}{b_4}$. Thus, from (31), the tracking error e converges to the ultimate bound of $\sqrt{\frac{2b_5}{b_1 b_4}}$ which can be made arbitrarily small via adjusting the control gains.

V. Numerical Studies

To demonstrate the effectiveness of the proposed control method, a comprehensive simulation study was conducted using the MATLAB/Simulink environment. For a realistic representation, the EHS was modeled using the Moog D633-R02K01M0NSM2 valve and the Hoerbiger LB6-1610-0080-4M piston. The model parameters were selected based on the experimental setup in [1], with the following values: $m = 3[kg]$, $b = 2200[Ns/m]$, $k = 0[Nm]$, $A_p = 2.01 \times 10^{-4}[m^2]$, $F_L = 0[Nm]$, $\beta_e = 7 \times 10^8[Pa]$, $V_t = 1.74 \times 10^{-5}[m^3]$, $C_{tl} = 2.5 \times 10^{-11}$, $C_d = 0.62$, $\omega = 2.04 \times 10^{-5}[m]$, $\rho = 850[kg/m^3]$, $p_s = 40[bar]$. As described in Section II, the control input u represents the valve's spool position and is constrained by its physical limits, thus saturating u to $\pm 7.9[mm]$ (*i.e.*, $u_l = -7.9[mm]$, $u_u = 7.9[mm]$). The neural network-based compensation term, designed in (26) was implemented as a single layer with z being its input and the hyperbolic tangent function, $\tanh(z)$, was used as the activation function. To improve the effective input range of the activation function, z , which has a pressure unit, was scaled by 1×10^{-5} before being processed. The estimated weight was initiated from zero.

In accordance with the piston's stroke length of $58[mm]$, a sinusoidal desired trajectory of the form $y_d = 28 + 24.5\sin(2\pi 0.1t - \pi/2)[mm]$ was implemented.

The gains of the proposed controller were selected as follows $k_e = 1$, $k_r = 8 \times 10^7$, $k_z = 1.5 \times 10^{-4}$, $\gamma_w = 1 \times 10^{-4}$, $k_w = 0.1$. The parameters of the bounds of f_r and f_z, which were introduced in (15) and (22), respectively, were selected as $\rho_r = 4 \times 10^3$, $\rho_z = 1$ and $\epsilon_r = 1 \times 10^{-3}$, $\epsilon_z = 1 \times 10^{-6}$.

To illustrate the effectiveness of the proposed method in enhancing trajectory tracking performance under the presence of actuator saturation nonlinearity, simulations were conducted for two cases: with and without the neural network component $\hat{\bar{\delta}}$ in the control scheme. The corresponding results are presented in Figures 1-7. Figure 1 and Figure 2 depict the trajectory tracking error e and control signal u along with $\mathrm{sat}(u)$, for the proposed controller. It is clear that satisfactory tracking performance is achieved even tough the control input is saturated. The variation of $\hat{w}$ over time is presented in Figure 3. The tracking error e and the control input, when the neural network compensation is removed from the proposed method, are shown in Figure 4 and Figure 5, respectively. Examination of these figures reveal that somewhat similar performance to that of the proposed controller is obtained.

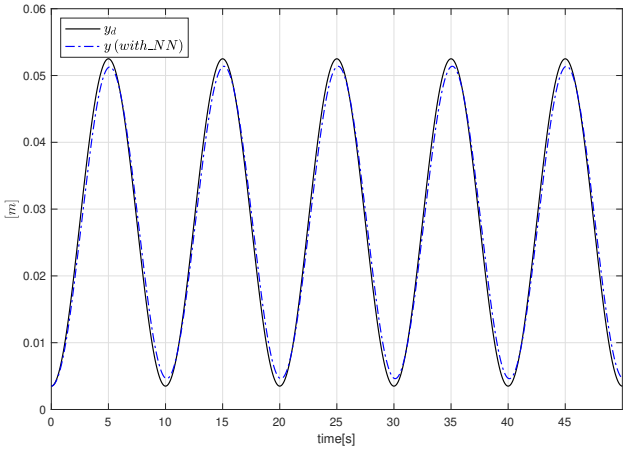

Fig. 1. Trajectory tracking performance y vs y_d (proposed control algorithm)

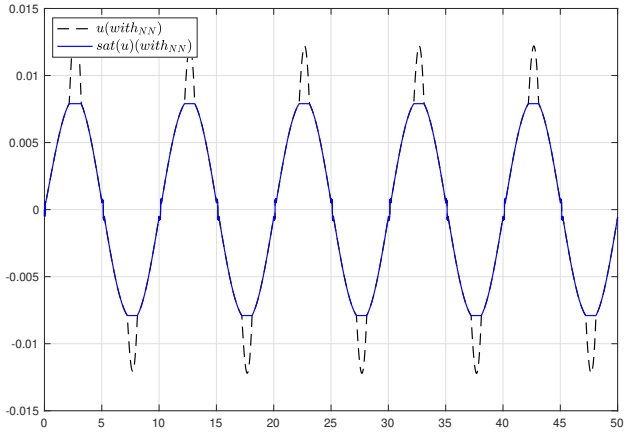

Fig. 2. Control signal (proposed control algorithm)

To further compare the results of the two cases, the tracking errors and the control signals u are presented,

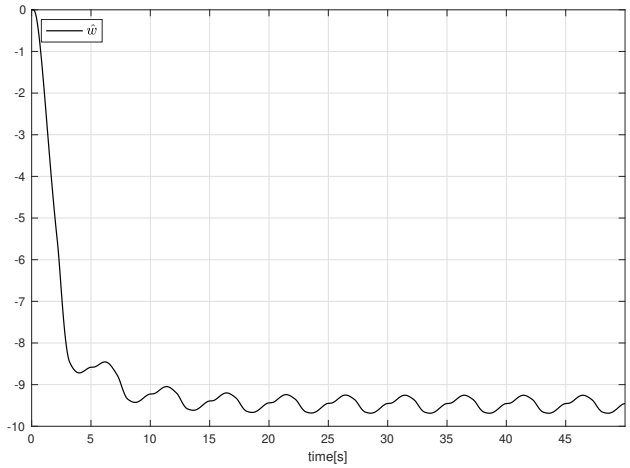

Fig. 3. The time evolution of $\hat{w}$ (proposed control algorithm)

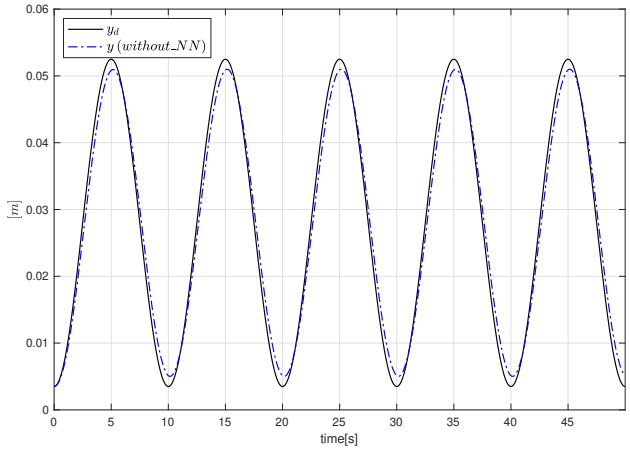

Fig. 4. Trajectory tracking performance y vs y_d (without neural network)

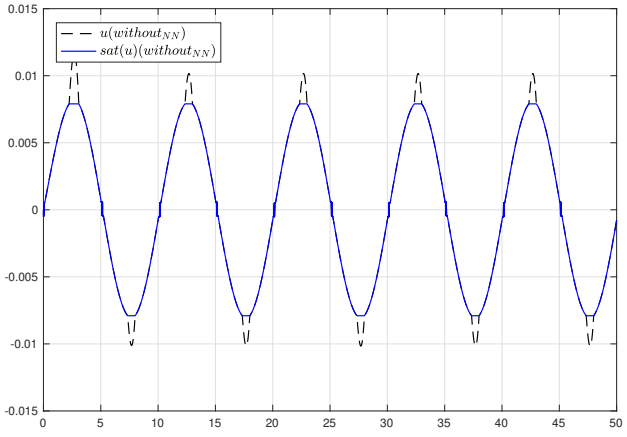

Fig. 5. Control signal (without neural network)

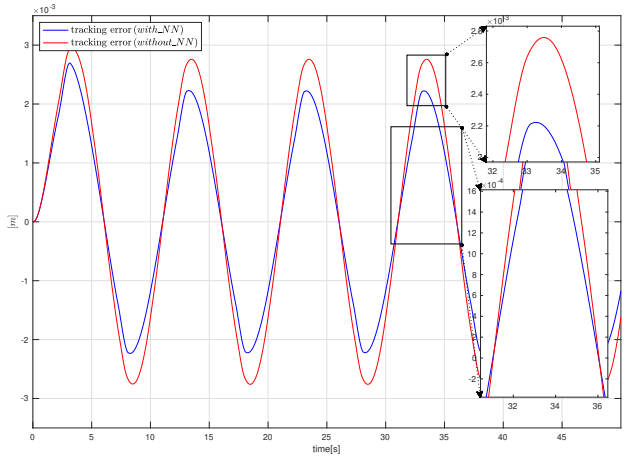

Fig. 6. Comparison of the tracking error for both cases

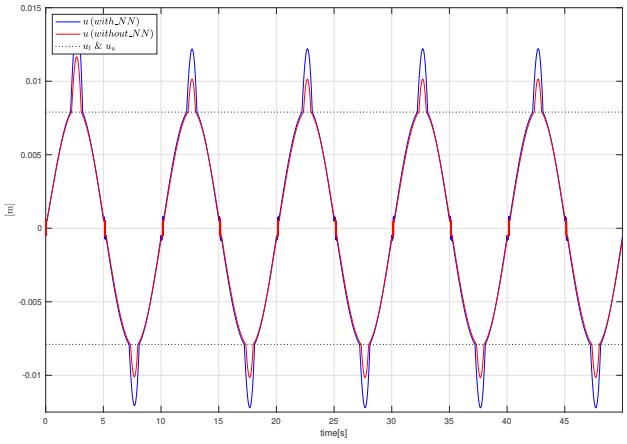

Fig. 7. Comparison of the control signal for both cases

respectively, in Figure 6 and Figure 7, for both cases. A closer investigation of these figures reveal that, in both cases, successful trajectory tracking is achieved when the control signal is within its saturation limits. However, when the control signals are outside the saturation limits, the tracking error increases in both cases. Specifically, examining Figure 6 reveals that the neural network component improves tracking accuracy even when the control signal is within its limits and significantly mitigates the effects of actuator saturation nonlinearity when it occurs. This improvement is further evident in the zoomed-in plots of Figure 6, where the proposed controller demonstrates enhanced tracking performance when the control signal reside within its limits. In an attempt to quantify these, the maximum tracking error is calculated between 22^{nd} and 23^{rd} seconds, when the control signal is higher than its upper limit. Specifically, thanks to the proposed controller, the maximum tracking error is reduced from $2.83[mm]$ to $2.27[mm]$, thus successfully compensating for the saturation-induced tracking error by 19.78%.

VI. Conclusions

We have presented the design and corresponding analysis of a robust backstepping type controller formulation based on neural network compensation for the displacement tracking problem of EHSs with uncertainties associated with its dynamical terms and actuator saturation. The proposed

formulation guarantees the uniform practical stability of the system states and ensures that the tracking error signal is uniformly ultimately bounded. Simulation studies performed using the actual parameter of an EHS are presented in order to illustrate the feasibility of the proposed method. Future work will concentrate on experimental verifications.

ACKNOWLEDGMENT

This study was supported by Scientific and Technological Research Council of Türkiye (TÜBİTAK) under the Grant Number 123E023 and 2210-C M.Sc. program. The authors thank to TÜBİTAK for their supports.

REFERENCES

[1] Q. Guo and D. Jiang, *Nonlinear Control Techniques for Electro-Hydraulic Actuators in Robotics Engineering*, CRC Press, 2017.

[2] K. K. Ahn, D. N. C. Nam, and M. Jin, "Adaptive backstepping control of an electrohydraulic actuator," *IEEE/ASME Transactions on Mechatronics*, vol. 19, no. 3, pp. 987–995, 2014.

[3] W. Kim, D. Won, D. Shin, and C. C. Chung, "Output feedback nonlinear control for electro-hydraulic systems," *Mechatronics*, vol. 22, pp. 766–777, 2012.

[4] Q. Guo, T. Yu, and D. Jiang, "High-gain observer-based output feedback control of single-rod electro-hydraulic actuator," *IET Control Theory and Applications*, vol. 9, pp. 2395–2404, 10 2015.

[5] Q. Guo, J. Yin, T. Yu, and D. Jiang, "Saturated adaptive control of an electrohydraulic actuator with parametric uncertainty and load disturbance," *IEEE Transactions on Industrial Electronics*, vol. 64, no. 10, pp. 7930–7941, 2017.

[6] N. Ye, J. Song, and G. Ren, "Model-based adaptive command filtering control of an electrohydraulic actuator with input saturation and friction," *IEEE Access*, vol. 8, pp. 48252–48263, 2020.

[7] C. Wang, J. Wang, Q. Guo, Z. Liu, and C.P. Chen, "Disturbance observer-based fixed-time event-triggered control for networked electro-hydraulic systems with input saturation," *IEEE Transactions on Industrial Electronics*, 2024.

[8] K. Young Ho and F. L. Lewis, *High-level feedback control with neural networks*, World Scientific, 1998.

[9] F. L. Lewis, S. Jagannathan, and A. Yesildirak, *Neural network control of robot manipulators and non-linear systems*, CRC press, 2020.

[10] K. Hornik, M. Stinchcombe, and H. White, "Multilayer feedforward networks are universal approximators," *Neural networks*, vol. 2, no. 5, pp. 359–366, 1989.

[11] F. L. Lewis, "Nonlinear network structures for feedback control," *Asian Journal of Control*, vol. 1, no. 4, pp. 205–228, 1999.

[12] M. Krstic, I. Kanellakopoulos, and P. V Kokotovic, *Nonlinear and adaptive control design*, Wiley, 1995.

[13] S. Unver, E. Selim, E. Tatlicioglu, E. Zergeroglu, and M. Alci, "Adaptive control of bldc driven robot manipulators in task space," *IET Control Theory & Applications*, 2024.

[14] D. Braganza, W. E Dixon, D. M. Dawson, and B. Xian, "Tracking control for robot manipulators with kinematic and dynamic uncertainty," *International Journal of Robotics & Automation*, vol. 23, no. 2, pp. 117–126, 2005.